Energetics of glutamate receptor ligand binding domain dimer assembly are modulated by allosteric ions

Charu Chaudhry[a], Andrew J. R. Plested[a,1], Peter Schuck[b], and Mark L. Mayer[a,2]

[a]Laboratory of Cellular and Molecular Neurophysiology, Porter Neuroscience Research Center, National Institute of Child Health and Human Development, and [b]Dynamics of Macromolecular Assembly, Laboratory of Bioengineering and Physical Science, National Institute of Biomedical Imaging and Bioengineering, National Institutes of Health, Department of Health and Human Services, Bethesda, MD 20892

Edited by Christopher Miller, Brandeis University, Waltham, MA, and approved June 4, 2009 (received for review April 15, 2009)

The activity of many ligand-gated ion channels and cell surface receptors is modulated by small molecules and ions, but an understanding of the underlying molecular mechanisms is scarce. For kainate, but not AMPA subtype glutamate receptors, the binding of Na^+ and Cl^- ions to discrete, electrostatically coupled sites in the extracellular ligand binding domain (LBD) dimer assembly regulates the rate of entry into the desensitized state, which occurs when the dimer interface ruptures and the channel closes. Studies on glutamate receptors have defined the LBD dimer assembly as a key functional unit that controls activation and desensitization. Here we use analytical ultracentrifugation to probe the energetic effects of allosteric ions on kainate receptor dimer stability in solution, using a GluR6 mutant that desensitizes slowly. Our results show that sodium and chloride ions modulate kainate receptor dimer affinity as much as 50-fold, and that removal of either Cl^- or Na^+ disrupts the dimer. The applicability of a similar allosteric mechanism for modulation of delta2 glutamate receptors by Ca^{2+} was also tested. Our results indicate that ions can contribute substantial free energy to active state stabilization in both these receptors, and provide quantitative measurements of the energetic consequences of allosteric ion binding to a ligand-gated ion channel.

allosteric modulation | analytical ultracentrifugation | desensitization | ion channels | thermodynamics

Allosteric regulation of ligand-gated ion channels (LGICs), is ubiquitous, involving discrete transitions between resting, conducting, and desensitized states, driven by agonist binding in symmetrical or pseudosymmetrical oligomeric structures (1). Small molecules, which bind at specific sites, have also been reported to act as allosteric modulators in all of the major LGIC families, namely glutamate receptors (2, 3), P2X receptors (4), and Cys-loop receptors (5). Many such allosteric modulators have potential use as therapeutics since their site of action is not restricted to the ligand-binding site or ion conduction pore, allowing design of compounds specifically targeted to particular receptor subtypes. Of interest, activity at different LGIC families is also modulated by extracellular ions including protons, calcium, chloride, copper, sodium, and zinc ions. Of these LGICs, perhaps the best studied are kainate subtype glutamate receptors which require both extracellular Na^+ and Cl^- for normal receptor activity (6, 7). Crystallographic studies reveal that these ions bind at physically discrete allosteric sites in the extracellular ligand-binding domain (LBD) by which they regulate receptor desensitization (8, 9).

Given detailed knowledge of the underlying molecular mechanisms, kainate receptors constitute a model system to understand the energetic principles governing allosteric modulation of LGICs by ions. Within the canonical model of glutamate receptor gating, the LBD dimeric assembly, which forms a dimer of dimers in the full-length tetrameric receptor, constitutes a crucial structural unit, conformational changes in which drive the channel through resting, conducting, and desensitized states (2, 10–12). Following release of the neurotransmitter glutamate by the presynaptic cell, receptors in the postsynaptic cell bind glutamate in a cleft between 2 domains (D1 and D2) of the "clamshell shaped" LBD formed by S1 and S2 polypeptide segments. Receptors activate through rotation of D2 and clamshell closure. A critical D1 inter-subunit interface forms between protomers of a dimer pair, allowing domain closure to place a torque on the ion channel and open it; this D1 interface forms the active dimer assembly. When the channel is open, the dimer is under strain. In the desensitized state, in which the pore shuts with glutamate still bound, the D1 interface breaks (2, 13). A plausible hypothesis for the role of Na^+ and Cl^- in the gating cycle of a kainate receptor is that the ions act to stabilize the active dimer assembly (8, 9). Such an ion-dependent allosteric mechanism is supported by the fact that, in the absence of monovalent inorganic ions, disulfide crosslinked kainate receptors show normal activation with no subsequent desensitization by glutamate, conditions under which wt GluR6 is strongly inhibited (8, 9, 14).

Although this hypothesis explains many aspects of ion modulation it has never been directly tested. Such a test requires measurement of the effects of monovalent ions on LBD dimerization, which so far has been precluded by failure of wt GluR6 to dimerize appreciably in solution (14). Here we circumvent this problem by using the GluR6 HERLK mutant receptor, which has a re-engineered dimer interface that enhances S1S2 dimerization and greatly slows desensitization (15). Using analytical centrifugation (AUC) and this mutant, we dissect the energetic effects of allosteric anions and cations on kainate receptor dimer stability in solution. In addition, we address the generality of this model of ion action for Ca^{2+} modulation of the orphan glutamate receptor delta2 that crystallizes as a dimer which binds Ca^{2+} ions (16). Our results indicate that allosteric ions contribute substantial free energy to stabilization of the active dimer assembly in both kainate and δ2 receptors. We postulate that in contrast to AMPA receptors the dimer interface may be intrinsically weak to allow for ion modulation in these receptors.

Results

Anion- and Cation-Binding Sites in GluR6 HERLK. We previously crystallized both wt GluR6 S1S2 (PDB 3G3F) and the HERLK mutant (PDB 3G3J) in the presence of NaCl, and in complex with glutamate, capturing active dimer assemblies at 1.4- and 1.3-Å resolution, respectively (15). In the mutant structure, the sequence of 5 amino acids in helices forming the dimer interface was switched

Author contributions: C.C., A.J.R.P., and M.L.M. designed research; C.C., A.J.R.P., P.S., and M.L.M. performed research; C.C., A.J.R.P., and P.S. analyzed data; and C.C., A.J.R.P., P.S., and M.L.M. wrote the paper.

The authors declare no conflict of interest.

This article is a PNAS Direct Submission.

[1]Present address: Leibniz-Institut für Molekulare Pharmakologie (FMP), Robert-Roessle-Strasse 10, 13125 Berlin, Germany.

[2]To whom correspondence should be addressed. E-mail: mlm@helix.nih.gov.

This article contains supporting information online at www.pnas.org/cgi/content/full/0904175106/DCSupplemental.

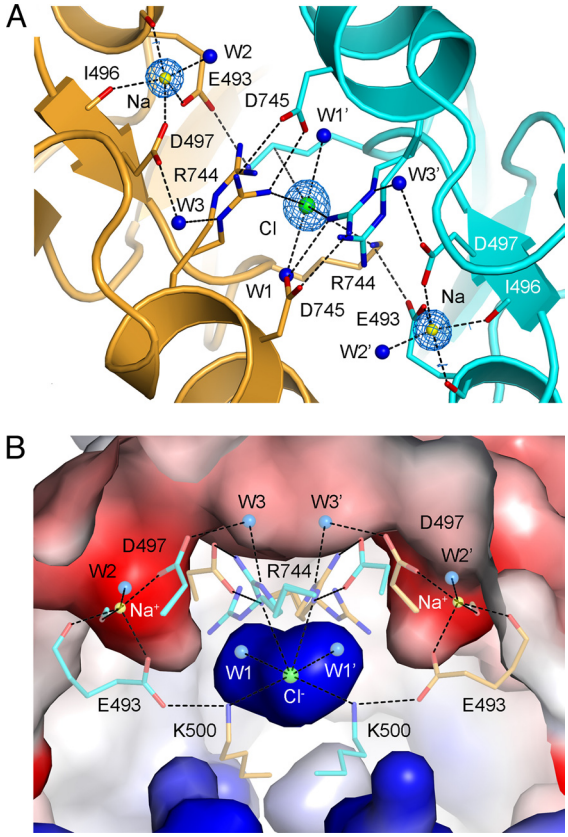

Fig. 1. The Na^+ and Cl^- binding sites in GluR6 HERLK. (*A*) Crystal structure of the 1.3 Å resolution glutamate complex (PDB 3G3J) looking down the molecular 2-fold onto the membrane plane; the 2 subunits of the dimer are colored gold and cyan. σ A-weighted 2mFo-DFc electron density maps contoured at 2σ are shown for Na^+ (yellow spheres) and Cl^- (green sphere) ions. (*B*) Electrostatic potential map of the protein interior contoured from −10kT/e (red) to +10kT/e (blue); view is rotated ≈90° from that in *A*. Side chains and solvent forming the pentavalent Na^+ and octahedral Cl^- coordination spheres are shown; the electrostatic potential map was calculated for the high occupancy conformation of R744.

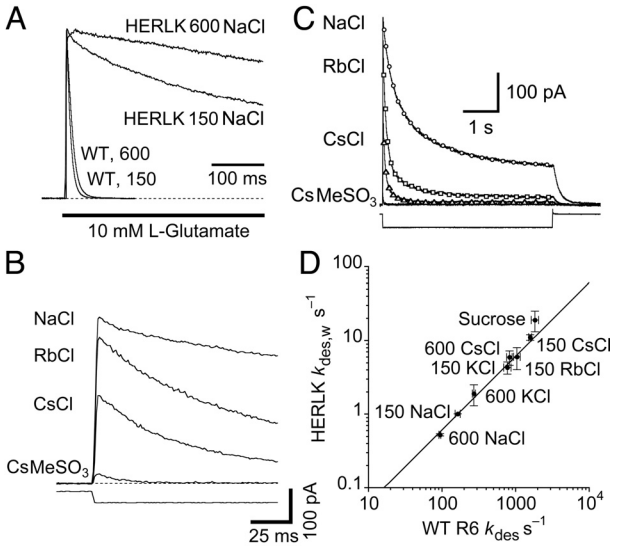

Fig. 2. Ion sensitivity of GluR6 HERLK resembles that for wt. (*A*) The kinetics of entry into desensitization are slowed for both wt GluR6 and HERLK when NaCl is increased from 150 to 600 mM. The glutamate application was 100 ms for wt and 7 s for HERLK. (*B*) Modulation of HERLK currents by cations and anions; the current is almost entirely abolished in $CsMeSO_3$. (*C*) The desensitization of HERLK currents is well described by 2 exponential decays for a range of ionic conditions. (*D*) Rates of entry into desensitization for wild-type and HERLK mutant receptors show a linear correlation across the entire range of ionic conditions tested ($R = 0.99$).

to the sequence found in the GluR2 L483Y mutant AMPA receptor in an attempt to recreate a non-desensitizing phenotype (2, 15). Electron density maps for the ion binding sites in GluR6 HERLK S1S2 reveal peaks at positions corresponding to a Cl^- ion on the D1 dimer interface, flanked by a pair of Na^+ ions, one in each subunit (Fig. 1*A*), as found previously for GluR5 dimer crystal structures with the partial agonist kainate (8, 9). Comparison of all atom rmsd values for the 6-residue loop forming the ion coordination spheres, after least squares superposition using D1 Cα coordinates, shows that the structures are nearly identical (rmsds 0.50 and 0.67 Å for the pair of subunits in the GluR5 dimer, and 0.27 and 0.44 Å for GluR6 HERLK, both compared with wt GluR6). These results establish that the rigid interconnected ion binding site structure, with the Na^+ ions ≈8 Å away from the Cl^- ion, and 15 Å away from each other, is conserved in different kainate receptor subtypes and not altered by the HERLK mutant (17).

Each of the Na^+ ions sits in a solvent-exposed electronegative pocket forming 5-fold coordination with the backbone carbonyl and side chain carboxylate of Glu-493, the backbone carbonyl of Ile-496, the side chain carboxylate of Asp-497, and a water molecule. The Cl^- ion, which binds in an electropositive cavity, shows 6-fold coordination with the pair of 2-fold related Lys-500 ammonium groups and the pair of Arg-744 guanidinium groups, along with 2 equatorial water molecules (Fig. 1*B*). Notably, side chains, comprising the ion coordination complexes in wt GluR6, the HERLK mutant, and GluR5, show negligible differences in torsion angles with the exception of Arg-744, which exhibits conformational variability (9). In GluR6 HERLK S1S2, Arg-744 forms a bidentate intermolecular salt-bridge with Asp 745 on helix J of its partner subunit, but also adopts an alternative conformation resulting from rotations of 40° and 100° for $\chi 2$ and $\chi 3$ that break the intermolecular salt-bridge and open up the anion site. The dynamic behavior of Arg-744 was also observed in molecular dynamics simulations for wt GluR5 suggesting a role in an entry or exit pathway for the Cl^- ion (17). A water-mediated contact between Asp-487, which binds the Na^+ ion, and Arg-744, which binds the Cl^- ion, is also remarkably conserved in the series of GluR5 and GluR6 crystal structures. These collective interactions provide a simple structural mechanism by which the bound ions are able to allosterically influence each other's binding and stabilize the dimer interface geometry.

Allosteric Ions Modulate GluR6 HERLK Desensitization. Because the Na^+ and Cl^- ion-binding sites were intact in the GluR6 HERLK mutant, we next examined if ion modulation of desensitization resembles that in wt GluR6, in which the allosterically coupled binding of Na^+ and Cl^- ions to the LBD reduces the rate of onset of desensitization (9). We measured the desensitization rate (k_{des}) of GluR6 HERLK in a range of external ionic conditions (Fig. 2). At physiological NaCl concentrations of 150 mM, HERLK desensitizes at a rate of 1.5 ± 0.2 s^{-1}; in contrast wt GluR6 desensitizes 110-fold faster, k_{des} 165 ± 14 s^{-1}. When extracellular NaCl is increased to 600 mM, a close to saturating concentration (EC_{50} 28 mM), the rate of desensitization slows 1.8-fold, to 94 ± 3 s^{-1} for wt (9), while for HERLK the rate slows 2.9-fold, to 0.52 ± 0.02 s^{-1}. By contrast, when extracellular Na^+ is replaced by equimolar concentrations of different monovalent cations, both wt GluR6 and HERLK show accelerated desensitization, with rates for 150 mM K^+, Rb^+ and Cs^+ of 780 ± 90 s^{-1}, 1,053 ± 111 s^{-1}, and 1,587 ± 76 s^{-1} for wt GluR6, and 4.3 ± 0.8 s^{-1}, 6 ± 2 s^{-1}, and 11 ± 1 s^{-1} for HERLK. For 600 mM K^+ and Cs^+ the rates were 273 ± 12 s^{-1} and 833 ± 70 s^{-1} for wt GluR6, and 1.9 ± 0.6 s^{-1} and 6 ± 1 s^{-1}

for HERLK. When Na^+ was replaced by Cs^+, concurrent with replacement of Cl^- by $MeSO_3^-$, the rate of desensitization for HERLK increased 50-fold, to 77 ± 7 s^{-1} whereas responses for wt GluR6 were too small to reliably measure. When both Na^+ and Cl^- were replaced by 246 mM sucrose k_{des} increased 20-fold for wt GluR6 (1,850 ± 200 s^{-1}), and 36-fold for HERLK (19 ± 6 s^{-1}) compared with values recorded in 600 mM NaCl. When the desensitization rates for HERLK are plotted versus those of wt GluR6, the data are well fit with a straight line (R = 0.99), indicating that the various ionic conditions produce identical perturbations in the 2 species. The slope of the fit is 0.006, meaning that on average the HERLK mutations slow desensitization by 165-fold, independent of the ionic conditions. These results provide strong evidence that the effects of ion binding and the HERLK mutations on the rate of desensitization are independent and separable. Thus, GluR6 HERLK provides a valid background to analyze the energetic effects of allosteric ion binding on dimer stability using direct physical measurements.

Allosteric Ion Effects on the Energetics of Dimerization. We previously used AUC to determine that with 165 mM NaCl GluR6 HERLK S1S2 dimerizes with a K_d of 102 μM (95% confidence interval 85–135 μM), a concentration at which the ion-binding sites are not fully occupied based on functional experiments (9, 15). To investigate the extent to which Na^+ and Cl^- ions stabilize the dimeric state, we carried out both sedimentation equilibrium (SE) and velocity (SV) experiments at a close to saturating concentration of NaCl (600 mM) and in its absence. In the latter test, the cation is replaced with Cs^+ and the anion with $MeSO_3^-$, conditions under which wt GluR6 currents are strongly inhibited (9), whereas for HERLK only a small rapidly desensitizing current is observed (Fig. 2).

Sedimentation profiles from SV experiments were analyzed by the c(s) size distribution method implemented in SEDFIT (18), using loading protein concentrations from 0.1–2 mg/mL (Fig. 3*A*). In 165 mM $CsMeSO_3$, the major peak has a weight-average sedimentation coefficient s_w of 2.6 S that was independent of loading concentration and close to the value previously measured for the wt GluR6 S1S2 monomer (14), indicating the absence of self-association. In sharp contrast, c(s) distributions in 600 mM NaCl exhibit broad peaks that are shifted toward higher s_w values of 3.5 S at 0.3 mg/mL and 3.7 S at 2 mg/mL. In prior experiments, we established a value of 4 S for disulfide cross linked GluR6 S1S2 dimers, indicating that 600 mM NaCl shifts the monomer-dimer equilibrium strongly toward the dimeric state. Notably, when the NaCl concentration is decreased to 165 mM, the s_w value at 2 mg/mL decreases to 3.3 S consistent with incomplete occupancy of the ion binding sites at physiological ion concentrations.

We next performed SE experiments acquiring multiple data sets at different initial protein concentrations and speeds to accurately determine equilibrium K_d for dimer formation under the 2 extreme conditions of 600 mM NaCl and 165 mM $CsMeSO_3$. We carried out a global nonlinear least squares analysis using SEDPHAT (18, 19), applying first-order corrections for the contribution of preferential solvation to the buoyant molar mass of the protein in high cosolvent conditions (*SI Materials and Methods*). An example of an equilibrium gradient from one representative dataset in 600 mM NaCl is shown in Fig. 3*B*. At 600 mM NaCl, the K_d for dimer formation was 12 μM (95% confidence interval 11–13 μM). In $CsMeSO_3$, there is a precipitous drop in the dimer fraction with a corresponding K_d of 550 μM (95% confidence interval 440–660 μM), which translates to a 2.1 kcal/mol loss of dimer stability due to the detrimental effect of NaCl removal. Thus, Na^+ and Cl^- modulate dimer affinity as much as 50-fold, supporting the proposed model of allosteric ion modulation of the dimeric LBD assembly.

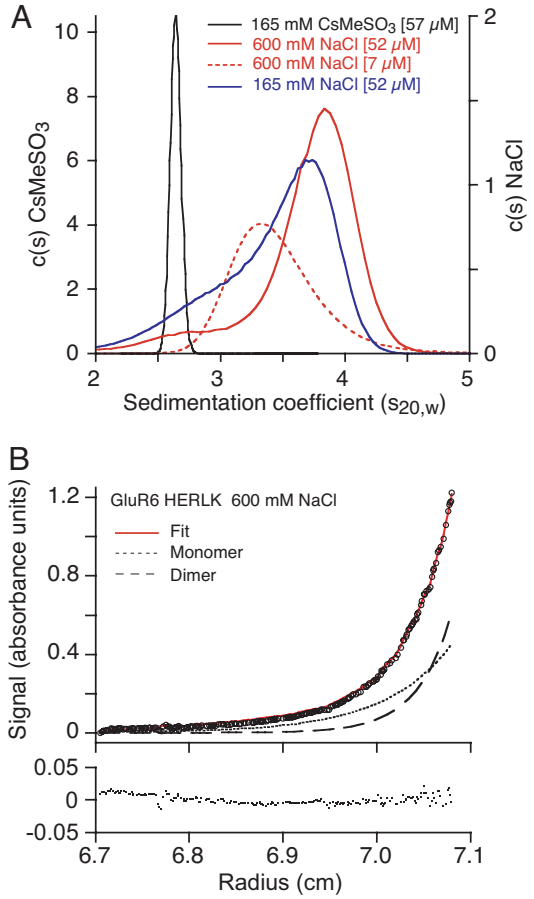

Fig. 3. Na^+ and Cl^- ions modulate LBD dimer stability. (*A*) Sedimentation velocity c(s) distributions for GluR6 HERLK in 165 and 600 mM NaCl (blue and red traces) and 165 mM $CsMeSO_3$ (black traces); values in brackets indicate protein concentrations calculated from integration of the c(s) distributions. In $CsMeSO_3$, the protein is monomeric (2.6S). 600 mM NaCl, the profile, reflecting a rapidly interconverting monomer-dimer system, shifts to s_w values of NB approximately 3.5 and 3.7S at loading concentrations of 0.3 and 2 mg/mL (dashed and solid red lines, respectively), approaching the expected 4S value for a dimer. (*B*) Representative sedimentation equilibrium distribution of HERLK in 600 mM NaCl at 24,000 rpm. Global fits to a monomer-dimer model yields a K_d of 12 μM (95% confidence interval of 11–13 μM). (*Upper*) Circles are the data points, the red line is the global fit, and dotted and dashed lines are the exponentials representing monomer and dimer fractions whose sum gives rise to this fit; (*Lower*) residuals are shown.

Individual Contributions of the Anion and Cation to Dimer Stability. We next tested the individual roles of the anion and cation species in dimer stabilization. For this experiment, we replaced Cl^- by the inorganic anion $MeSO_3^-$, which in functional experiments produces rapidly desensitizing responses (8). In separate experiments Na^+ was replaced by the chloride salt of the large organic cation N-methyl-D-glucamine ($NMDG^+$), which also speeds desensitization (9). The effects on dimer formation was analyzed using SE. Strikingly, in both cases dimer formation was strongly inhibited. Fig. 4 *A* and *B* show representative equilibrium gradients used in the respective global analyses, which yielded a K_d of 610 μM (95% confidence interval 450–890 μM) for $NaMeSO_3$ and 550 μM (95% confidence interval 510–600 μM) for NMDG-Cl. In each case, the free energy of dimer dissociation decreases by ≈2 kcal/mol. Thus, both Cl^- and Na^+ play a crucial role in dimer energetics for kainate receptors.

Ca^{2+} Modulates Dimer Affinity for GluR Delta2 Ligand-Binding Domains. At the time the ion binding sites were discovered in kainate receptors, no similar sites had been reported for any of

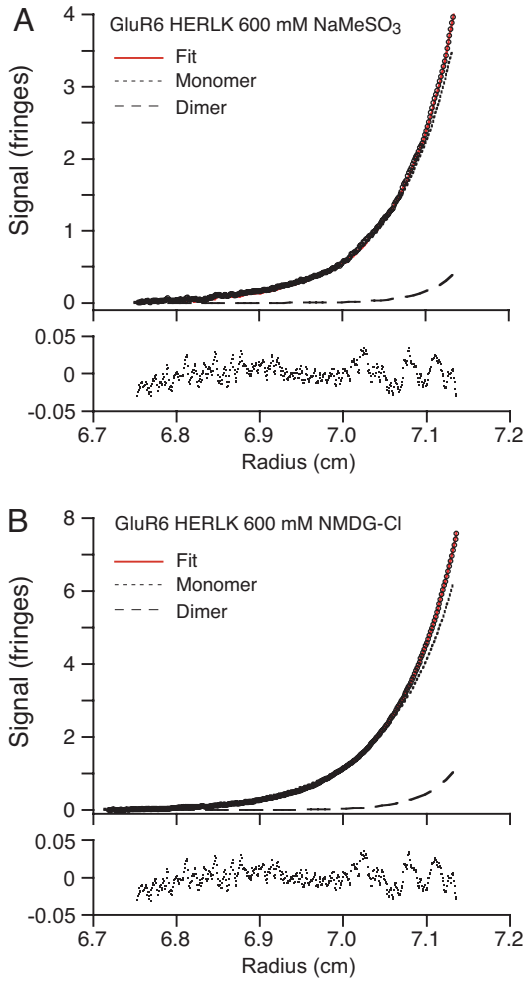

Fig. 4. Dimer assembly is disrupted on removal of either anion or cation. Representative sedimentation equilibrium profiles for GluR6 HERLK at 24,000 rpm with Cl^- replaced by $MeSO_3^-$ (*A*) and Na^+ by $NMDG^+$ (*B*). The dimerization K_d decreases about 50-fold in both cases yielding values of 610 μM (95% confidence interval of 450–890 μM) for $NaMeSO_3$ and 550 μM (510–600 μM) for NMDG-Cl.

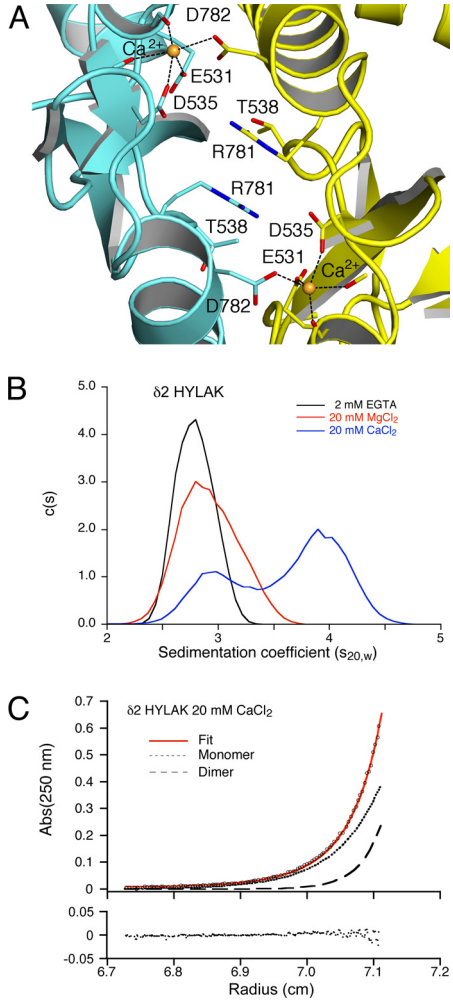

Fig. 5. Ca^{2+} stabilizes the active dimer assembly in GluR δ2. (*A*) Top view of the GluRδ2-S1S2 dimer structure (PDB 2V3T) showing 2 bound Ca^{2+} ions (gold spheres) forming pentavalent coordination complexes that link the dimer assembly (16, 23). Side chains for R781 and T538, equivalent to R744 and K500 in GluR6, are shown to highlight the absent anion site. (*B*) Sedimentation coefficient distributions of HYLAK δ2 yields S_w values of 3.42S in 20 mM $CaCl_2$ (2.4 mg/mL), 2.76S in 20 mM $MgCl_2$ (2.5 mg/mL), and 2.69S in 2 mM EGTA (2.4 mg/mL); protein concentrations are derived from integrated peaks in c(s) distributions. (*C*) Representative sedimentation equilibrium distribution of HYLAKδ2 in 20 mM $CaCl_2$ derived from a global analysis of data at 3 concentrations and 3 rotor speeds, using a monomer-dimer model with a K_d of 62 μM (95% confidence interval of 51–74 μM). Graph shows data points at 24,000 rpm, the black line is the model used to fit the data, and dotted and dashed lines represent the best-fit populations of monomer and dimer respectively; residuals of the fit are shown below the graph.

the other glutamate receptors of known structure, including AMPA receptors (2), NMDA receptor NR1 subunits, NR1/NR2 heterodimers (20), and NMDA receptor NR3 subunits (21); all of these receptors lack the electrostatic hot spots that bind Na^+ and Cl^- in GluR5 and GluR6. Thus it came as a surprise when a crystal structure of the iGluR orphan delta2 subunit in the apo state revealed a dimer with 2 Ca^{2+} ions bound at the dimer interface (Fig. 5*A*), at a similar location to monovalent cations in kainate receptors (16). However, before this result was published, electrophysiological measurements had revealed that Ca^{2+} acts as a positive allosteric modulator for GluR δ2 containing the lurcher mutation in the 2nd transmembrane segment of the ion channel (A654T, GluRδ2^{Lc}). Currents through GluRδ2^{Lc} ion channels exhibit robust Ca^{2+} dependent potentiation that is voltage-independent, and insensitive to intracellular BAPTA, suggesting an underlying site of Ca^{2+} action not within the membrane electric field but on the extracellular protein face (22). Based on these reports, we previously suggested that much like cation modulation in kainate receptors, Ca^{2+} regulates dimer stability of δ2 receptor ligand binding domains, and that this stabilization is the mechanism by which Ca^{2+} facilitates functional activity (9). A more recent study showing that engineered disulfide bonds that crosslink the δ2 dimer interface mimic the functional effects of extracellular Ca^{2+} on receptor activity supports this hypothesis (23). The prediction then would be that Ca^{2+} regulates the monomer-dimer equilibrium of δ2 S1S2 much like Na^+ regulates kainate receptor dimer assembly.

To test this prediction, we performed AUC experiments using purified δ2 S1S2. However, similar to wt GluR6, we failed to observe any effects of Ca^{2+} on δ2 S1S2 oligomerization assayed by analytical gel filtration coupled to light scattering, refractive index, and UV measurements, which showed that wt δ2 does not oligomerize to an appreciable extent even at 10 mg/mL. Because the δ2, GluR2, and GluR6 S1S2 ligand-binding domains all have similar folds and crystallize as dimers, we reasoned that dimer interface engineering, which proved successful in the GluR6 HERLK mutant, might enable us to study Ca^{2+} induced effects on δ2 dimer-

ization. Accordingly, using structure based sequence alignments, we created the δ2 "HYLAK" mutant by introducing a tyrosine into helix D of δ2 in place of P638, along with mutations of 4 neighboring residues in helices B, D, and J to their AMPA receptor counterparts, in an attempt to recreate the high-affinity binding site for the Tyr side chain found in the non desensitizing GluR2 L483Y mutant (2). On helix J, mutation of Q786 to a leucine and E790 to a lysine is expected to permit favorable inter-subunit van der Waals and cation-π interactions with the aromatic ring of P638Y in helix D, whereas mutation of R787 in helix J to an alanine restores electrostatic charge balance in the region. On helix B, mutation of Y591 to a histidine is expected to remove a potentially competing intramolecular cation-π interaction with E790K and instead prime the Lys side chain to form the crucial intermolecular cation-π interaction with P638Y (Fig. S1).

The δ2 HYLAK mutant ligand binding domain protein was purified and studied by SV and SE. The δ2 monomer and dimer have standard s-values of 2.7 S, measured experimentally at low protein concentrations, and 4.33 S, estimated using the dimer mass increase with the 2:3-power rule, respectively; these values are consistent with the theoretical sedimentation coefficients calculated using HYDROPRO (24). C(s) distributions derived from SV experiments in different ion conditions show that Ca^{2+} produces a striking concentration dependent rightward shift in s_w value, in contrast to Mg^{2+} which has virtually no effect. The s_w values for EGTA, 20 mM Ca^{2+} and 20 mM Mg^{2+} were 2.69, 3.42, and 2.76 (Fig. 5*B*). Consistent with these results, currents in GluRδ2^{Lc} are potentiated by Ca^{2+} but not Mg^{2+} (22, 23), underscoring a specific requirement for Ca^{2+}. Subsequent SE analyses establish that in the presence of 20 mM $CaCl_2$, the K_d for dimer formation is 62 μM, 95% confidence interval 51–74 μM (Fig. 5*C*). By contrast, in 2 mM EGTA or 20 mM Mg^{2+}, the K_d weakens substantially to 1.1 mM (95% confidence interval 0.6–3.2 mM) and 1.0 mM (95% confidence interval 0.6–2.5 mM), respectively, corresponding to ≈1.6 kcal/mole loss of dimer stability (Fig. S2). At a Ca^{2+} concentration of 2 mM, the K_d for dimer formation was 520 μM (95% confidence interval 320–1,000 μM), suggesting that at physiological concentrations the Ca^{2+}-binding sites are not saturated (Fig. S2).

Discussion

It is well-established that ion channel gating is exquisitely sensitive to the ionic milieu of the cell. Specifically, there is extensive literature on the functional effects of permeant ions on channel gating, dating back to the first example in synaptic channels such as the acetylcholine receptor, where slowed channel closing in the presence of high concentrations of permeant ions was observed (25). In potassium channels, the hypothesis that permeant ions stabilize the open channel structure (26) was established directly by crystallographic analysis (27). More recent reports provide evidence that nonpermeant ions also regulate the gating machinery of many LGICs through allosteric modulation at sites outside the ion channel pore, but the underlying molecular mechanisms are in most cases poorly understood.

In this work, we study the effects of allosteric ion binding to the extracellular ligand binding domains of kainate and δ2 receptors. Using AUC to probe the influence of ion binding on the energetics of LBD dimerization, our results show that sodium and chloride ions in the case of kainate receptors, and calcium ions in the case of δ2, stabilize the D1 dimer interface and modulate affinity of the dimer assembly, as much as 50- and 18-fold respectively. The molecular basis for this mechanism is revealed in crystal structures of ion-bound complexes showing that either 2 Na^+ and a Cl^- ion or 2 Ca^{2+} ions bound to discrete sites stabilize the active dimer assemblies (9, 23). In functional studies on GluR6, removal of external ions accelerates D1 dimer breakage, that is, desensitization, reflecting reduced stability of the dimer assembly. Ions do not affect the rates of recovery from desensitization (8, 9) because in models of the GluR6 desensitized state, captured crystallographically in AMPA receptors using D2 disulfide trapped mutants (13), the D1 interface is reorganized, which disrupts the anion- and cation-binding sites. Together our data support the notion that allosteric anions and cations bound to discrete sites in the LBD are integral components of kainate and δ2 receptors, and that they alter D1 dimer energetics, providing comprehensive structural, functional, and energetic characterization of modulation of a LGIC by allosteric ions.

Kainate receptors are unique amongst iGluRs in that both external anions and cations strongly modulate their desensitization kinetics and dimer affinity. Electrophysiological studies reveal that AMPA receptor responses do not exhibit this behavior (6), and we observed no effect of ions on GluR2 L483F dimer assembly assayed by light scattering and analytical size exclusion chromatography (Fig. S3). By contrast, δ2^{LC} receptor ion channel activity is solely Ca^{2+} dependent (22, 23). Because each of these iGluR subtypes have a similar dimer arrangement with similar buried surface areas, it is expected that they share a conserved gating mechanism in which stability of the D1 dimer interface is inversely correlated to the rate and extent of desensitization. Nonetheless, their dimer interfaces vary in the details of intermolecular interactions providing important mechanistic insight.

On first inspection, the central location of the bound Cl^- in an electropositive pocket at the GluR6 D1 interface, suggests it may provide the critical electrostatic glue that brings the monomers together in contrast to the flanking structurally coupled Na^+ ions. Strikingly, however, replacement of Na^+ with $NMDG^+$, or replacement of Cl^- with $MeSO_3^-$, resulted in a comparable energetic destabilization of the dimer assembly. Insight into the underlying mechanism comes from the results of computational studies investigating the free energy landscape or potential of mean force (PMF) along a defined reaction coordinate for the Cl^- ion (17). This calculation revealed that the presence of cations lowers the electrostatic field above the surface of the buried anion cavity, providing a more energetically favorable path for anion approach and binding. However, in the δ2 receptor the anion-binding site is obliterated by replacement of the residue equivalent to Lys-500, which binds the Cl^- ion in GluR6, with a threonine side chain (16, 23). To fill the void, Arg-781 in δ2 rotates by 90° along the molecular 2-fold compared with the conformation of Arg-761 in GluR6, to occupy a position deeper in the cavity (Fig. 5*A*). This rotation causes Asp-782, the equivalent of Asp-761 in GluR6, to be released from an intermolecular salt bridge, and thus come within binding distance of the Ca^{2+} ion.

The cation binding site in the δ2 receptor thus comprises 4 protein ligands from 1 subunit, generated by carbonyl and carboxylate groups of Glu-531, Val-534, and Asp-535, while the fifth ligand is generated by the carboxyl group of Asp 782 in the partner unit. The Ca^{2+} ion thus acts as intermolecular electrostatic "glue" that holds the pair of subunits in a dimer assembly together. By contrast, in kainate receptors all of the protein contacts with Na^+ are made by a single subunit and a water molecule occupies the fifth coordination position (Fig. 1*A*). In δ2, the contribution of Asp-782 likely switches selectivity from monovalent to divalent ions by creating a binding site with a higher field strength, which was also achieved in the GluR6 M739D mutant (28), with the key difference from δ2 that all of the ion ligands are present in a single GluR6 subunit. In functional studies on full length δ2^{LC} the EC_{50} for Ca^{2+} potentiation is 200 μM, whereas our AUC results suggest a lower affinity. This difference likely results from the formation of the Ca^{2+}-binding site at an inter subunit interface, due to an avidity effect produced by the high local concentration of δ2 subunits, which occurs in a tetrameric receptor assembly confined to the plane of the lipid bilayer, an effect absent in biophysical studies on isolated δ2 S1S2 in solution.

It is noteworthy that dimer formation by the wt kainate and δ2 receptor S1S2 ligand binding domains is too weak to measure by AUC, and that we had to use the subterfuge of dimer interface

engineering to bring the K_d of the dimers into a range experimentally accessible with this approach. Despite the profound functional effects of allosteric ions on the rate of desensitization of kainate receptors measured using electrophysiological techniques, the question thus arises as to whether ion modulation of dimer stability is indeed functionally significant, as we propose. In fact, the weak interaction energy of the ligand binding domain dimers in intact wt glutamate receptors is critical for allowing fast signaling, and the low affinity for dimer formation is compensated by the approximate 10^3 fold increase in receptor subunit concentration that occurs when oligomeric proteins are confined to the 2-dimensional plane of the lipid bilayer (29). Furthermore, "intrinsic" dimer stability in the absence of bound allosteric ions, as measured by the rate of desensitization in 246 mM sucrose, is 15-fold faster in GluR6 subtype kainate receptors ($1{,}850 \pm 200\ s^{-1}$) than for their AMPA receptor counterparts ($126\ s^{-1}$), which are not strongly modulated by allosteric ions (6, 8, 9, 30). Since k_{des} is inversely related to the energetic barrier of D1 dimer breakage, the 15-fold faster rate of desensitization of kainate receptors in the absence of ions compared with that of AMPA receptors implies that a kainate D1 dimer assembly is less stable by ≈2 kcal/mol versus its AMPA receptor counterpart. We postulate that the weaker dimer interface in kainate receptors may indeed serve a functional role allowing modulation by ions. We suggest that the properties of intrinsic dimer stability and ion affinity are interrelated and finely tuned. Thus, much like permeant ions stabilize a metastable pore in many channels, allosteric ions may stabilize an inherently weaker LBD dimer interface in kainate and delta subtype glutamate receptors.

Materials and Methods

Mutagenesis and Protein Purification. HERLK GluR6 was overexpressed in *E. coli* and purified by using methods described in refs. 15 and 31. For GluRδ2, DNA sequences encoding S1 (Gly-440 to Arg-551) and S2 (Ser-664 to Leu-813) connected by Gly-Thr linker were expressed in Origami B (DE3) cells (Novagen) using a modified pET22 T7 expression vector. Cells were induced at OD600 = 1 with 30 μM IPTG, grown at 18 °C overnight, and the GluRδ2 protein was purified by using Ni-NTA resin, followed by removal of the N-terminal His-6 tag by trypsin cleavage, and final purification on a Q Sepharose column; 30 mM glycine was included in all purification steps. δ2 Y591H, P638Y, Q786L, R787A, and E790K mutations were made by overlap PCR and confirmed by sequencing the ORF.

Analytical Ultracentrifugation. A Beckman XL-I analytical ultracentrifuge with absorbance and Rayleigh interference optics was used to obtain SV and SE data. Before runs, samples were further purified by Superdex 200 gel filtration chromatography, concentrated, and dialyzed against 20 mM HEPES, pH 7.5, buffer containing for GluR6 HERLK 2 mM glutamate and either 165 mM NaCl, 600 mM NaCl, 600 mM $NaMeSO_3$, 600 mM NMDG-Cl, or 165 mM $CsMeSO_3$, and for δ2 HYLAK, 30 mM glycine, and either 2 mM EGTA, 2 mM $CaCl_2$, 20 mM $CaCl_2$, or 20 mM $MgCl_2$. For SV runs, different protein concentrations ranging from 0.1 to 4 mg/mL were loaded into double-sector cells, and profiles collected at 50,000 rpm and 20 °C. SE experiments were carried out for 0.1, 0.3, and 1 mg/mL samples at 4 °C and at multiple speeds (12, 18, and 24 K rpm) with both absorbance (230, 250, and 280 nm) and interference detection using sapphire windows, "aged" cell components, and water blank correction. SV and SE data were analyzed by using SEDFIT and SEDPHAT (18). Further details of analysis and error statistics are provided in *SI Materials and Methods*.

Electrophysiology. Wild-type and mutant kainate receptors were expressed in HEK cells for excised patch recording as previously described (9). The internal solution contained either 115 or 570 mM NaCl, and (in mM): 10 NaF, 0.5 $CaCl_2$, 1 $MgCl_2$, 5 Na_4BAPTA, 5 Hepes, and 10 Na_2ATP, pH 7.3. The external solution contained 0.1 mM each of $MgCl_2$ and $CaCl_2$ and in most cases 5 mM Hepes titrated to pH 7.3. We added 150 or 600 mM salts as required with sucrose to maintain osmolarity. We applied pulses of 10 mM glutamate to excised patches and recorded the patch current (filtered 1–5 kHz) using the program Synapse; for GluR6 HERLK responses, the rate of desensitization was calculated as the weighted sum of a 2 exponential fit: $k_{des,w} = (k_{des1} * amp1 + k_{des2} * amp2)/(amp1+amp2)$. This calculation was not necessary for wt GluR6 for which the second component was frequently too small to measure accurately. The solution exchange was typically complete in 400 μs, as confirmed after the experiment from junction currents. Fitting and plotting was done in Kaleidagraph (Synergy Software).

ACKNOWLEDGMENTS. We thank Carla Glasser for preparing cDNAs; Andrea Balbo for technical assistance with AUC experiments; and the National Institute of Neurological Disorders and Stroke DNA Sequencing Facility. This work was supported by the intramural research programs of National Institute of Child Health and Human Development, National Institutes of Health, Department of Health and Human Services (M.L.M) and National Institute of Biomedical Imaging and Bioengineering, National Institutes of Health, Department of Health and Human Services (P.S.); and the Helen Hay Whitney Foundation (C.C.).

1. Changeux JP, Edelstein SJ (1998) Allosteric receptors after 30 years. *Neuron* 21:959–980.
2. Sun Y, et al. (2002) Mechanism of glutamate receptor desensitization. *Nature* 417:245–253.
3. Jin R, et al. (2005) Mechanism of positive allosteric modulators acting on AMPA receptors. *J Neurosci* 25:9027–9036.
4. Silberberg SD, Li M, Swartz KJ (2007) Ivermectin interaction with transmembrane helices reveals widespread rearrangements during opening of P2X receptor channels. *Neuron* 54:263–274.
5. Ymer S, et al. (1990) Structural and functional characterization of the gamma 1 subunit of GABAA/benzodiazepine receptors. *EMBO J* 9:3261–3267.
6. Bowie D (2002) External anions and cations distinguish between AMPA and kainate receptor gating mechanisms. *J Physiol* 539:725–733.
7. Paternain AV, Cohen A, Stern-Bach Y, Lerma J (2003) A role for extracellular Na+ in the channel gating of native and recombinant kainate receptors. *J Neurosci* 23:8641–8648.
8. Plested AJ, Mayer ML (2007) Structure and mechanism of kainate receptor modulation by anions. *Neuron* 53:829–841.
9. Plested AJ, Vijayan R, Biggin PC, Mayer ML (2008) Molecular basis of kainate receptor modulation by sodium. *Neuron* 58:720–735.
10. Armstrong N, Gouaux E (2000) Mechanisms for activation and antagonism of an AMPA-sensitive glutamate receptor: Crystal structures of the GluR2 ligand binding core. *Neuron* 28:165–181.
11. Mayer ML, Olson R, Gouaux E (2001) Mechanisms for ligand binding to GluR0 ion channels: Crystal structures of the glutamate and serine complexes and a closed apo state. *J Mol Biol* 311:815–836.
12. Nanao MH, Green T, Stern-Bach Y, Heinemann SF, Choe S (2005) Structure of the kainate receptor subunit GluR6 agonist-binding domain complexed with domoic acid. *Proc Natl Acad Sci USA* 102:1708–1713.
13. Armstrong N, Jasti J, Beich-Frandsen M, Gouaux E (2006) Measurement of conformational changes accompanying desensitization in an ionotropic glutamate receptor. *Cell* 127:85–97.
14. Weston MC, Schuck P, Ghosal A, Rosenmund C, Mayer ML (2006) Conformational restriction blocks glutamate receptor desensitization. *Nat Struct Mol Biol* 13:1120–1127.
15. Chaudhry C, Weston MC, Schuck P, Rosenmund C, Mayer ML (2009) Stability of ligand-binding domain dimer assembly controls kainate receptor desensitization. *EMBO J* 28:1518–1530.
16. Naur P, et al. (2007) Ionotropic glutamate-like receptor delta2 binds D-serine and glycine. *Proc Natl Acad Sci USA* 104:14116–14121.
17. Vijayan R, Plested AJ, Mayer ML, Biggin PC (2009) Selectivity and cooperativity of modulatory ions in a neurotransmitter receptor. *Biophys J* 96:1751–1760.
18. Schuck P (2000) Size-distribution analysis of macromolecules by sedimentation velocity ultracentrifugation and lamm equation modeling. *Biophys J* 78:1606–1619.
19. Vistica J, et al. (2004) Sedimentation equilibrium analysis of protein interactions with global implicit mass conservation constraints and systematic noise decomposition. *Anal Biochem* 326:234–256.
20. Furukawa H, Singh SK, Mancusso R, Gouaux E (2005) Subunit arrangement and function in NMDA receptors. *Nature* 438:185–192.
21. Yao Y, Harrison CB, Freddolino PL, Schulten K, Mayer ML (2008) Molecular mechanism of ligand recognition by NR3 subtype glutamate receptors. *EMBO J* 27:2158–2170.
22. Wollmuth LP, et al. (2000) The Lurcher mutation identifies delta 2 as an AMPA/kainate receptor-like channel that is potentiated by Ca(2+). *J Neurosci* 20:5973–5980.
23. Hansen KB, et al. (2009) Modulation of the dimer interface at ionotropic glutamate-like receptor delta2 by D-serine and extracellular calcium. *J Neurosci* 29:907–917.
24. Garcia De La Torre J, Huertas ML, Carrasco B (2000) Calculation of hydrodynamic properties of globular proteins from their atomic-level structure. *Biophys J* 78:719–730.
25. Ascher P, Marty A, Neild TO (1978) Life time and elementary conductance of the channels mediating the excitatory effects of acetylcholine in Aplysia neurones. *J Physiol* 278:177–206.
26. Baukrowitz T, Yellen G (1996) Use-dependent blockers and exit rate of the last ion from the multi-ion pore of a K+-channel. *Science* 271:653–656.
27. Zhou Y, Morais-Cabral JH, Kaufman A, MacKinnon R (2001) Chemistry of ion coordination and hydration revealed by a K+ channel-Fab complex at 2.0 A resolution. *Nature* 414:43–48.
28. Plested AJ, Mayer ML (2009) Engineering a high-affinity allosteric binding site for divalent cations in kainate receptors. *Neuropharmacology* 56:114–120.
29. Luckey M (2008) *Membrane Structural Biology: With Biochemical and Biophysical Foundations* (Cambridge Univ Press, New York).
30. Horning MS, Mayer ML (2004) Regulation of AMPA receptor gating by ligand binding core dimers. *Neuron* 41:379–388.
31. Mayer ML (2005) Crystal structures of the GluR5 and GluR6 ligand binding cores: Molecular mechanisms underlying kainate receptor selectivity. *Neuron* 45:539–552.